Journal of Biochemical and Molecular Toxicology

WILEY

RESEARCH ARTICLE

ALYREF Promotes Pyroptosis in Severe Acute Pancreatitis by Inhibiting the Activation of ATK/mTOR Signaling Pathway Through m5C Modification on AKT1

Jinlong Wei[1] | Zhenglin Zhang[1] | Jin Wang[1] | Wen Jiang[1] | Long Qian[1] | Maoming Xiong[2]

[1]Department of Third Surgery, Wuhu Hospital of Traditional Chinese Medicine, Wuhu, Anhui, China | [2]Department of General Surgery, First Affiliated Hospital of Anhui Medical University, Hefei, Anhui, China

Correspondence: Maoming Xiong (13955389811@163.com)

Received: 23 June 2025 | **Revised:** 22 September 2025 | **Accepted:** 22 November 2025

Funding: This study was supported by the 2024 Wuhu Science and Technology Bureau Project (2024kj095).

Keywords: AKT/mTOR | ALYREF | m5C modification | pyroptosis | severe acute pancreatitis

ABSTRACT

Severe acute pancreatitis (SAP) is a digestive system disease with a high mortality rate. Acinar cell pyroptosis is crucial for the pathogenesis of SAP, but its mechanism has not been fully elucidated. m5C modification is involved in the progression of multiple diseases, but its role in SAP remains unclear. In this study, we aimed to investigate the mechanism of pyroptosis in SAP mediated by m5C modification. *In vivo* and in vitro SAP model were established by inducement of caerulein and cholecystokinin on C57BL/6 mice and 266-6 cells. Hematoxylin eosin staining, TUNEL assay, ELISA, flow cytometry and western blot were performed to evaluate levels of inflammation and pyroptosis in vivo and in vitro of SAP. The underlying mechanism was detected by dot blot, methylated RNA Immunoprecipitation (MeRIP), RIP, dual luciferase reports and immunofluorescence staining. Results showed that inflammation and pyroptosis were increased in in vivo and in vitro SAP models, with the enhancement of m5C modification and ALYREF expression. Moreover, ALYREF knockdown inhibited inflammatory infiltration of pancreatic tissue and pyroptosis in the SAP mouse and cell models. ALYREF knockdown enhanced AKT1 expression by decreasing m5C modification on AKT1, and activated AKT/mTOR signaling pathway, while inhibiting the activation of AKT/mTOR pathway reversed the inhibition of pyroptosis induced by ALYREF knockdown. Collectively, we demonstrated that ALYREF knockdown inhibited pyroptosis in SAP through activating AKT/mTOR signaling pathway by decreasing m5C modification on AKT1. This study may provide a novel target and basis for the treatment of SAP.

1 | Introduction

Acute pancreatitis is an inflammatory condition of the pancreas that is mild in most patients and resolves within a week [1]. About 20–30% patients may develop severe acute pancreatitis (SAP), with a mortality rate of up to 15% [2]. SAP is characterized by rapid onset and severe disease, with consist organ failure and metabolic disorder, including respiratory failure, renal failure, cardiovascular failure and systemic inflammatory response syndrome and is the leading causes of death in patients with SAP [3, 4]. With the intensive research on SAP, several therapeutic drugs for SAP have been developed, reducing systemic reactions and mortality in patients [5, 6]. However, the pathogenesis of SAP has not been fully elucidated and still needs further investigation.

Recent studies have revealed that the mechanisms of SAP involve microcirculatory disturbances, intestinal barrier dysfunction, and an imbalance in cell death modalities [7–9]. Notably, pyroptosis has been demonstrated to influence the severity of SAP and its

associated lung and intestinal injury [10, 11]. Pyroptosis is a type of programmed cell death mediated by gasdermin (GSDM), which is characterized by continuous swelling, expansion, and rupture of cells, leading to the release of cellular contents and inflammatory factors, thereby activating a series of inflammatory responses [12, 13]. Pyroptosis has proven to be a double-edged sword. Moderate pyroptosis promotes the release of pathogen by eliminating infected cells and enhances immune activity to effectively clear pathogens [14, 15]. On the contrary, excessive pyroptosis aggravates the inflammation in the body and the damage of tissue cells, exacerbating the progression of the disease [16, 17]. Pyroptosis is closely associated with progression of multiple diseases, including cancers, liver diseases, autoimmune disease and cardiovascular disease [18–21]. Recently, several studies revealed that pyroptosis is involved in the pathogenesis of SAP, and the mechanism is complex [11, 22]. For instance, Wang et al. [23] found that the activation of the Akt/NF-κB and Caspase-3/GSDME pathways exacerbates acinar cell damage by enhancing pyroptosis. Furthermore, Lin et al. [24] demonstrated that S1PR2 triggers pyroptosis in intestinal epithelial cells via the RhoA/ROCK signaling pathway, thereby exacerbating intestinal injury and inflammation in SAP. Moreover, it has been demonstrated that inhibition of pyroptosis enhances the therapeutic outcomes in SAP. Therefore, studying the mechanism of pyroptosis of SAP may provide a new approach for the treatment of this disease.

RNA modification is one of the research hotspots in recent years, which is involved in regulating gene expression and controlling cell fate [25]. Among them, 5-methylcytidine (m5C) is a methylation modification occurs at position 5 of the cytidine residues of RNA and widely exists on tRNA, rRNA, mRNA [26]. m5C modification is catalyzed by NSUN family, removed by TET proteins and ALKBH1, and recognized by ALYREF, YBX1 and several proteins [27]. These proteins are involved in various biological functions by regulating RNA maturation, stability, output, and cellular translation [28, 29]. m5C modification is involved in the developmental disability, and the regulation of tumor immune microenvironment in cancer development [30–32]. Several studies used bioinformatic analysis to identify that m5C modification may mediate the progression of type 2 diabetes mellitus, rheumatoid arthritis and osteoarthritis by regulating pyroptosis [33, 34]. However, the mechanism by which m5C methylation regulates pyroptosis has not been adequately investigated, and whether it is involved in the development of SAP has not been reported

In this study, C57BL/6 mice were induced by caerulein to establish a SAP mouse model, and mouse pancreatic acinar carcinoma 266-6 cells were induced by cholecystokinin to establish an in vitro SAP model, and investigated the level of pyroptosis in vivo and in vitro models of SAP, as well as the mechanism by which m5C modification regulates pyroptosis in SAP. This study further understood the pathogenesis of SAP and may provide new insights into the prevention and treatment of SAP.

2 | Methods

2.1 | Animal Study

Animal study was approved by the Ethics Committee of Anhui College of Traditional Chinese Medicine (Approval number: KY-2024-027). Eight-week old C57BL/6 mice were maintained on a 12-h light/dark cycle at 22 ± 2°C for 1 week adaption with free access to food and water. Mice were randomly divided into the normal group, SAP group, SAP + KO-NC group and SAP + KO-ALYREF group (six mice/group). Lentiviral vector injection was conducted 1 day before induction of SAP mouse model. Mice in the SAP + KO-NC group and the SAP + KO-ALYREF group were injected with lentiviral vectors carrying short hairpin negative control (sh-NC) and shALYREF plasmids through the tail vein. SAP mouse model was induced by intraperitoneal (i.p.) injection of caerulein (200 μg/kg) at an hour interval for a total of 10 injections [35]. After inducement of SAP mouse model, mice were killed by 5% isoflurane. Part of pancreatic tissues were stored in −80°C for qPCR or western blot and the rest were fixed in 4% paraformaldehyde for histological analysis. Blood samples were obtained from the tail veins, and centrifuged at 2000 × *g* for 10 min to collect serums. The serums were stored at -80°C for further investigation.

2.2 | Cell Culture and Treatment

Mouse pancreatic acinar carcinoma 266-6 cells were purchased from American Type Culture Collection (Manassas, VA, USA). Cells were cultured in Dulbecco's modified eagle medium (Gibco, Grand Island, NY, USA) containing 10% fetal bovine serum (Gibco) and 1% penicillin-streptomycin at 37°C with 5% CO_2. To induce a SAP cell model, cells were treated with 8 μM cholecystokinin for 12 h. To inhibit the activation of AKT/mTOR signaling pathway, cells were induced with 20μmol/L AKT inhibitor GSK690693.

2.3 | Cell Transfection

Short hairpin RNA targeting ALYREF (sh-ALYREF) and shRNA negative control (shNC) were provided by GeneChem (Shanghai, China). 266-6 cells were seeded in a six-well plate, and the transfection was conducted when cell fusion reached 70–80% using Lipofectamine 2000 (Invitrogen, Carlsbad, CA, USA) according to the manufacturer's protocol. Cells were harvested after 48 h transfection.

2.4 | Hematoxylin Eosin (H&E) Staining

Mice pancreases fixed with 4% paraformaldehyde were dehydrated, embedded in paraffin, and made into 5 μm sections. The sections after dewaxing and hydrating were stained with hematoxylin for 5 min and eosin (Beyotime, Shanghai, China) for 30 s, respectively. The sections were dehydrated, transparent, sealed and observed under a microscope.

2.5 | Tunel Assay

TUNEL assay was performed using a TUNEL apoptosis assay kit (Beyotime). Paraffin sections after dewaxing were incubated with 20 μg/ml protease K not containing DNase for 15 min at room temperature for 15 min. Next, samples were incubated with biotin labeling solution for 1 h at 37°C, streptavidin-HRP

solution for 30 min and DAB solution for 20 min, respectively. The nucleus was stained with hematoxylin. The sections were observed under a microscope.

2.6 | ELISA

The levels of inflammatory factors IL-1β, IL-6 and TNF-α in the serum of mice were measured using the ELISA kits (Beyotime) according to the manufacturer's protocol. The absorbance was measured at 450 nm using a microplate reader.

2.7 | Detection of LDH Release

LDH release was detected using a LDH cytotoxicity assay kit (Beyotime). Cells were seed in a 96-well plate, and LDH release detection was performed according to the manufacturer's protocol when the cell fusion reached 80-90%. The absorbance was measured at 490 nm.

2.8 | Flow Cytometry

Apoptosis of 266-6 cells was detected using an Annexin V-FITC apoptosis detection kit (Beyotime). Cells of different groups were mixed with Annexin V-FITC and propyl iodide for 20 min protected from light at room temperature. Apoptosis was detected using a FACSCalibur cytometer (BD, Franklin Lakes, NJ, USA).

2.9 | Western blot

Total protein of mouse pancreatic tissues and 266-6 cells was isolated using radioimmunoprecipitation assay lysis buffer (Beyotime). Protein samples were quantified using a BCA kit (Beyotime) and loaded on 10% SDS-PAGE. After electrophoretic separation, the samples were transferred to PVDF membranes and incubated with 5% skim milk for 2 h block. The membranes were then incubated with anti-NLRP3 (ab263899, 1/1000, Abcam, Cambridge, MA, USA), anti-CASP1 (ab207802, 1/1000, Abcam), anti-p-AKT (ab38449, 1/1000, Abcam), anti-AKT (ab8805, 1/1000, Abcam), anti-p-mTOR (ab109268, 1/1000, Abcam), anti-mTOR (ab2732, 1/2000, Abcam) and anti-GAPDH (ab181602, 1/10000, Abcam) overnight at 4°C. Next, the membranes were incubated with secondary antibodies (ab6721, 1/10000, Abcam) for 2 h at room temperature. Blots were visualized using the enhanced chemiluminescence (ECL) reagent (Yeasen, Shanghai, China) and photographed with an optical luminescence instrument (GE, Chicago, IL, USA).

2.10 | Dot Blot Assay

RNA extraction of mouse pancreatic tissues and 266-6 cells was performed using Trizol reagent (Invitrogen). The RNA was denatured by heat and transferred onto a Hybond-N+ membrane (Solarbio, Beijing, China). Subsequently, the membrane was cross-linked with UV and blocked with 5% skim milk for 1 h. The membranes were incubated with anti-m5C overnight at 4°C followed by incubation with secondary antibodies (1: 10000, ab6721, Abcam) for 1 h. The membranes were visualized using ECL reagent. For internal standard detection, the membrane was incubated with 0.02% methylene blue (Sigma-Aldrich, St. Louis, MO, USA) in 0.3 M sodium acetate (pH 5.2) for 15 min.

2.11 | Quantitative Real-Time PCR (qPCR)

Extracted total RNA of mouse pancreatic tissues and 266-6 cells was reverse-transcribed into cDNA using a cDNA synthesis kit (Vazyme, Nanjing, China). qPCR was conducted using SYBR green master mix (Vazyme) on CFX96 system (Bio-Rad, Hercules, CA, USA). Relative mRNA expression was detected using the $2^{-\Delta\Delta Ct}$ method with GAPDH as the reference standard for normalization. The qPCR primers are presented in Table 1.

2.12 | Bioinformatic Analysis

The genes interacted with ALYREF were predicted using the GeneMANIA database (http://genemania.org/). The potential m5C sites of AKT1 were predicted using the RNAm5Cfinder database (http://www.rnanut.net/rnam5cfinder/).

2.13 | Rna Immunoprecipitation (RIP)

RIP assay was performed using a RIP assay kit (Beyotime) to detect the interaction between ALYREF and AKT1. Protein A/G Agarose was incubated with anti-AKT1 or anti-IgG for 30 min at room temperature. The pre-coated Protein A/G Agarose was centrifuged at 1000×g for 1 min at 4°C. The supernatant was discarded and incubated with cell lysate for 4 h at 4°C. Finally, the samples were eluted and purified, and AKT1 expression was measured by qPCR.

2.14 | Methylated RIP (MeRIP)

The m5C modification of AKT1 was measured using a m5C MeRIP kit (Cloudseq, Shanghai, China). RNA was fragmented using the fragmentation buffer on a PCR instrument at 70°C for 6 min. PMG beads were incubated with anti-m5C for 1 h at room temperature on a shaker. The beads were collected by centrifugation and resuspended in IP buffer. Next, fragmented RNA was incubated with PGM beads pre-coated with anti-m5C for 1 h at room temperature for IP. The RNA samples were purified according to the manufacturer's protocol, and the m5C modification of AKT1 was measured by qPCR.

2.15 | Rna Stability Assay

To detect the stability of AKT1 mRNA in 266-6 cells transfected with sh-NC and sh-ALYREF, cells were treated with 5 μg/mL actinomycin D (Merck, Darmstadt, Germany), and the expression of AKT1 was measured before and 4, 8 and 12 h after treatment by qPCR.

TABLE 1 | qPCR Primers.

Gene	Forward Primer	Reverse Primer
NOP2	CGAAAGGCCCGAAAACAGAAG	TGGATAACTCTCCAGGCAATGT
NSUN2	AGGTGGCTATCCCGAGATCG	GACTCCATGAATTGGTCCCATT
NSUN3	GACTCCATGAATTGGTCCCATT	AGGACTGTGTGATAGCCCCTC
NSUN6	AAGACAACAGGGTGAAGTGATTG	TCCATCAAATTCTTTGGCTCCTT
NSUN7	TCTCAAGGTGGTCTACCGAAA	TTCATTGCGTGTGTTAGCTGT
TRDMT1	GCGCTGCGAGAAAGTCATATC	CCCTGTAGGCCAATTCTTGTG
ALYREF	GGCACCGTACAGTAGACCG	AAGTCCAGGTTTGACACGAGC
TET1	GCAGTGAACCCCGGAAAAC	AGAGCCATTGTAAACCCGTTG
TET2	CTCCCATCAGCCATACAGAACC	CTGACTGTGCGTTTTATCCCT
TET3	TGCGATTGTGTCGAACAAATAGT	TCCATACCGATCCTCCATGAG

2.16 | Dual Luciferase Reports Assay

To identify the m5C site of AKT1, luciferase reporter plasmids wild type (wt)-AKT1 and mutation (mut)-AKT1 sequence containing predicted m5C sites sequences were constructed by cloning into the pGL3 vector. 266-6 cells were seeded in a 24-well plate and cotransfected with the luciferase reporter plasmids and sh-NC or sh-ALYREF for 48 h using Lipofectamine 2000. Dual-luciferase reporter assay system (Promega, San Luis Obispo, CA, USA) was performed to measure the luciferase activity.

2.17 | Immunofluorescence (If) Staining

The location of ALYREF and AKT1 in 266-6 cells was identified by IF staining using an IF staining kit (Beyotime). Cells were fixed in fixative for 10 min and blocked with sealing fluid for 60 min. Subsequently, cells were incubated with anti-AKT1 overnight at 4°C and then incubated with secondary antibodies for 1 h protected from light. The nuclei were stained with 4',6-diamidino-2-phenylindole (Beyotime) and cells were observed using a confocal microscope.

2.18 | Statistical Analysis

The data were analyzed using SPSS 22.0 software. The comparison between two or more groups was carried out by means of Student's *t* test or one-way analysis of variance (ANOVA), and results were expressed as mean ± standard deviation of at least three replicates. $p < 0.05$ was recognized as statistically significant.

3 | Results

3.1 | Inflammation Level and Pyroptosis Are Increased in the SAP Mouse Model and the Cell Model

To investigate the mechanism of SAP development, we evaluated the inflammation level and pyroptosis in SAP mouse model and cell model. H&E and TUNEL staining suggested that inflammatory cell infiltration and interstitial edema, as well as apoptotic cells were increased in pancreatic tissue of the SAP mouse model compared with the normal group (Figure 1A,B). Moreover, the levels of IL-1β, IL-6 and TNF-α were significantly increased in the SAP mouse model (Figure 1C–E). In vitro experiments suggested that LDH release, pyroptosis and the protein levels of NLRP3 and CASP1 were significantly increased in the SAP cell model (Figure 1F–H). In conclusion, these results demonstrated that the inflammation level and pyroptosis were increased in the SAP mouse model and the cell model.

3.2 | m5C Modification and ALYREF Expression Are Upregulated in the SAP Mouse Model and the Cell Model

To explore the function of m5C modification in SAP, we first detect the m5C level in the SAP mouse model and cell model. Results showed that the m5C levels were increased in the SAP mouse model and cell model (Figure 2A,B). Next, we measured the expression of several m5C-related genes in the SAP mouse model. Results suggested that the expression of NSUN2, NSUN3 and ALYREF was significantly upregulated in the SAP mouse model, especially ALYREF (Figure 2C). Meng et al. [36] demonstrated that circTMEM45A interacts with ALYREF to activate the NLRP3/caspase-1/IL-1β inflammatory pathway through m6A modification. Given that the core pathological mechanism of SAP involves NLRP3 inflammasome activation-driven pyroptosis and IL-1β-mediated inflammatory storm, this study provides direct mechanistic evidence supporting the selection of ALYREF as a key regulatory factor in SAP, thereby establishing it as the central target of our investigation. Moreover, the protein level of ALYREF in pancreatic tissues of SAP mouse model (Figure 2D), as well as ALYREF mRNA and protein levels in the SAP cell model were all upregulated (Figure 3E,F). Taken together, we demonstrated that m5C modification and ALYREF expression were upregulated in the SAP mouse model and the cell model¼.

3.3 | ALYREF Knockdown Inhibits the Pathological Changes of the Pancreas and Inflammation Level in the SAP Mouse Model

Subsequently, we evaluate the function of ALYREF in the SAP mouse model. qPCR suggested that ALYREF knockdown significantly reduced ALYREF mRNA expression and protein level in pancreatic tissues in the SAP mouse model (Figure 3A).

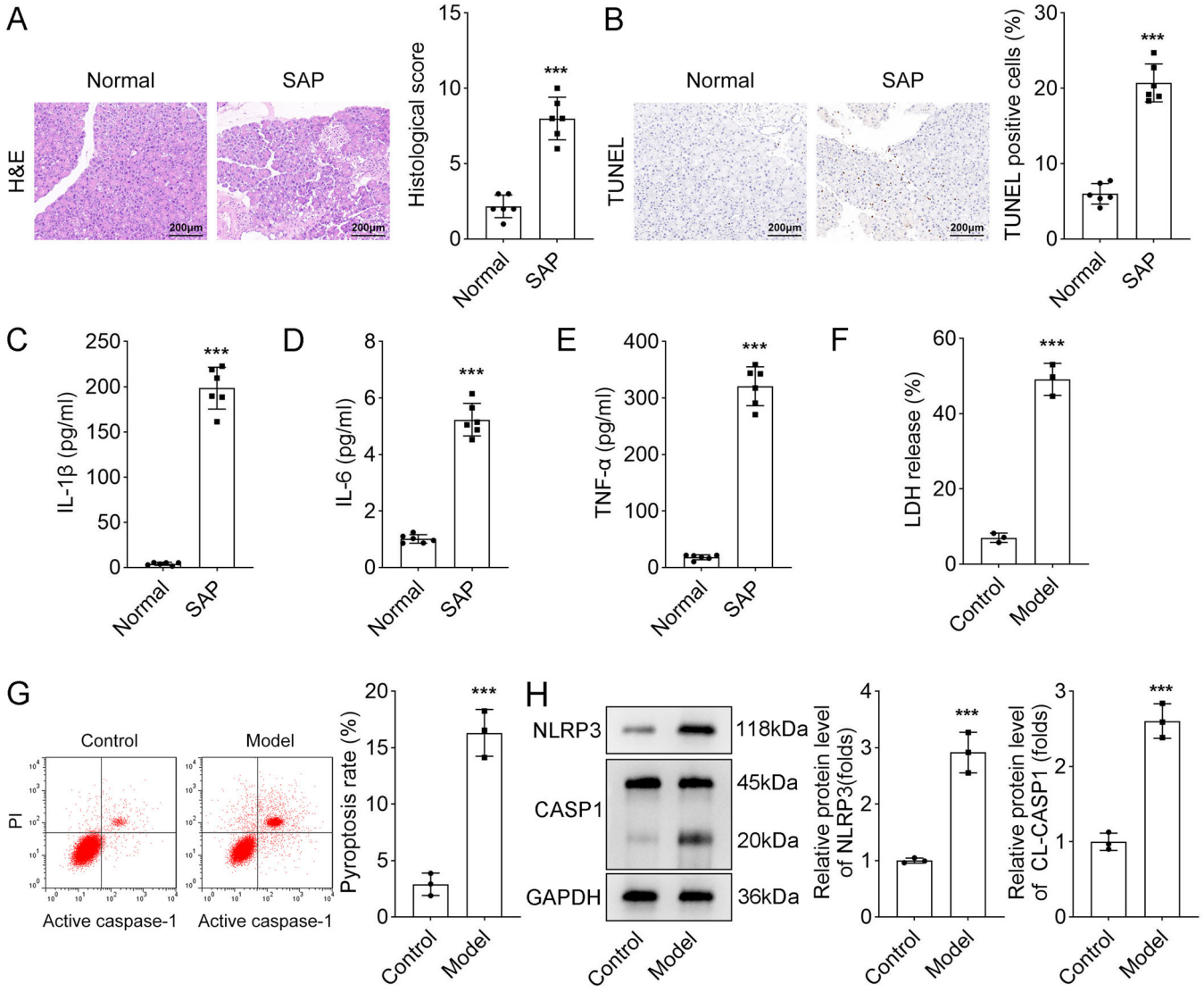

FIGURE 1 | Inflammation level and pyroptosis were increased in the SAP mouse model and the cell model. (A) Pathological change in pancreatic tissues of mice was detected by H&E staining. (B) The pyroptosis in pancreatic tissues of mice was evaluated by TUNEL assay. (C–E) The levels of IL-1β, IL-6 and TNF-α in serums of mice were measured using ELISA kits. (F) LDH release in 266-6 cells was detected using a LDH cytotoxicity assay kit. (G) Pyroptosis of 266-6 cells was evaluated by flow cytometry. (H) The protein levels of NLRP3 and CASP1 in 266-6 cells were detected by western blot. ***$p < 0.001$ versus the control group.

Compared with the SAP group, ALYREF knockdown ameliorated inflammatory cell infiltration, interstitial edema and tissue necrosis in pancreas (Figure 3C,D). Moreover, TUNEL staining suggested that ALYREF knockdown inhibited the number of apoptotic cells in the pancreatic tissues (Figure 3E). Moreover, the levels of inflammatory factors IL-1β, IL-6 and TNF-α in the SAP mouse model were significantly decreased by ALYREF knockdown (Figure 3F–H). Collectively, these results showed that ALYREF knockdown inhibited the pathological changes of the pancreas and inflammation level in the SAP mouse model.

3.4 | ALYREF Knockdown Inhibits Pyroptosis in the SAP Cell Model

Next, 266-6 cells were transfected with sh-ALYREF, and ALYREF mRNA expression and protein level were significantly decreased after transfection (Figure 4A,B). ALYREF knockdown also significantly reduced LDH release in the SAP cell model (Figure 4C). Moreover, the upregulated protein levels of NLRP3 and CASP1 in the SAP cell model were inhibited by ALYREF knockdown (Figure 4D). Additionally, ALYREF knockdown also suppressed pyroptosis increased in the SAP cell model (Figure 4E). In conclusion, we confirmed that ALYREF knockdown inhibited pyroptosis in the SAP cell model.

3.5 | ALYREF Knockdown Activates AKT/mTOR Signaling Pathway by Inhibiting the m5C Modification on AKT1

Then, we explored the mechanism of SAP regulated by ALYREF. Figure 5A presented several genes predicted to interact with ALYREF. We identified these genes through RIP

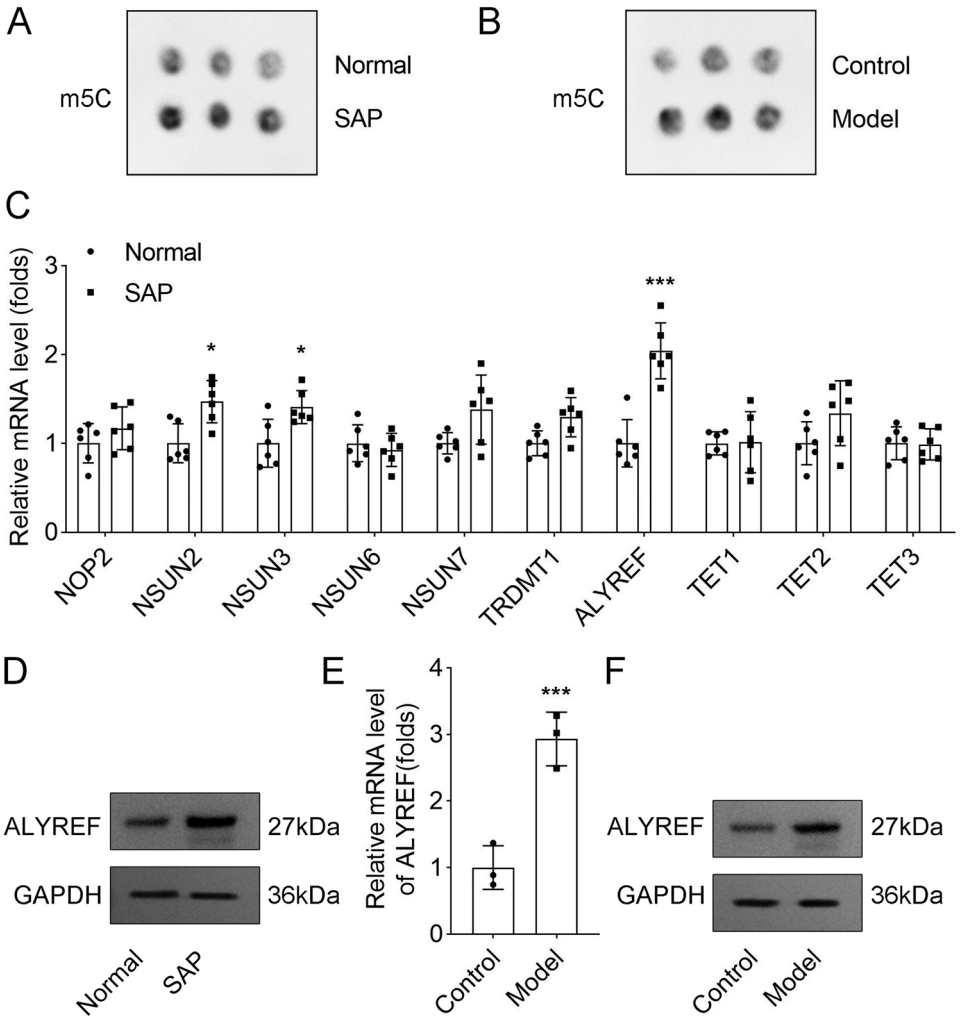

FIGURE 2 | m5C modification and ALYREF expression were upregulated in the SAP mouse model and the cell model. (A, B) The m5C levels in the SAP mouse model and cell model were detected by dot blot assay. (C) The expression of m5C-related genes in pancreatic tissue was measured by qPCR. (D) The protein levels of ALYREF in the SAP mouse model were detected by western blot. (E) ALYREF expression in 266-6 cells was measured by qPCR. (F) The protein levels of ALYREF in 266-6 cells were detected by western blot. $^{*}p < 0.05$ and $^{***}p < 0.001$ versus the control or normal group.

experiments and found that ALYREF interacted with AKT1 (Figure 5B). Moreover, ALYREF knockdown significantly decreased the m5C modification on AKT1 (Figure 5C), but increased the stability of ALYREF mRNA (Figure 5D). It has been demonstrated that ALYREF affects mRNA expression in a m5C-modified dependent manner [37]. These results suggested that ALYREF may mediate m5C methylation of AKT1 mRNA. To further elucidate the mechanism by which ALYREF regulates AKT1 m5C modification, we predicted several potential m5C sites of AKT1 mRNA, which were shown in Figure 5E. These sequences were cloned into luciferase reporter plasmids, and subsequently we identified the m5C methylation site of AKT1 by dual luciferase reporter assay. Results demonstrated that knockdown of ALYREF significantly enhanced the luciferase activity at site 1 and site 2, particularly at site 1, while it had no effect on the luciferase activity at site 3 and site 4 (Figure 5F). Additionally, IF staining showed overlap in localization of ALYREF and AKT1 (Figure 5G), further indicating an interaction between AKT1 and ALYREF. Additionally, ALYREF knockdown upregulated the protein level of AKT and increased the phosphorylation of AKT and mTOR, indicating that ALYREF knockdown activated AKT/mTOR signaling pathway (Figure 5H,I). Moreover, ALYREF knockdown downregulated the protein levels of NLRP3 and CASP1 (Figure 5J), indicating that ALYREF knockdown inhibited pyroptosis in 266-6 cells. Collectively, these results demonstrated that ALYREF knockdown activated AKT/mTOR signaling pathway by inhibiting the m5C modification on AKT1.

3.6 | Inhibition of the AKT/mTOR Signaling Pathway Activation Promotes Pyroptosis in the SAP Cell Model Inhibited by ALYREF Knockdown

There is evidence that the inactivation of AKT/mTOR pathway promotes pyroptosis in cancer and other diseases [38, 39]. Therefore, rescue experiments were performed to evaluate the role of AKT/mTOR signaling pathway in pyroptosis in SAP. AKT inhibitor GSK was treated on SAP cell model transfected with sh-ALYREF, and we found that GSK downregulated the levels of p-AKT, AKT and p-mTOR increased by ALYREF knockdown, suggesting that GSK inhibited the activation of SAP cell model with ALYREF

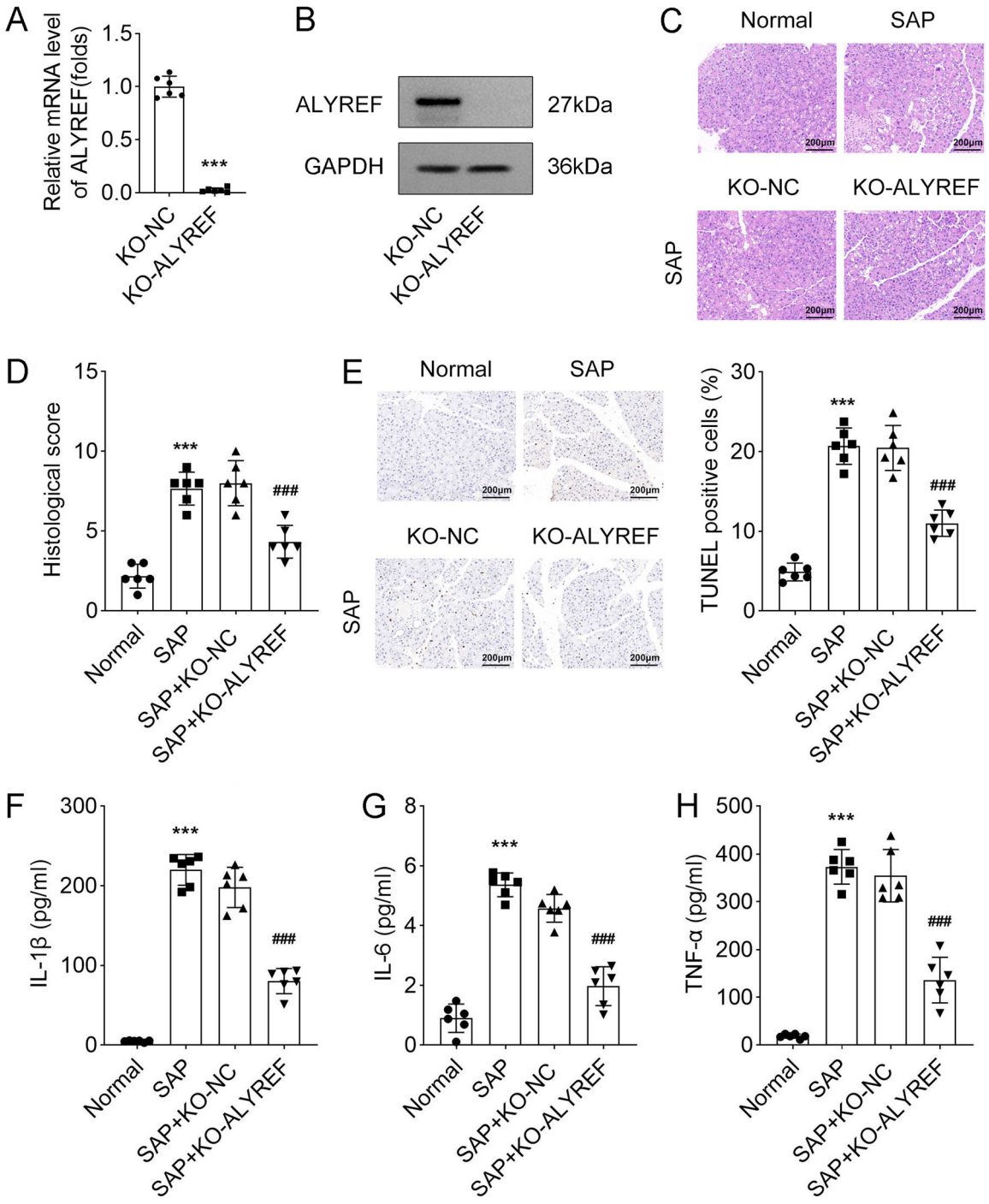

FIGURE 3 | ALYREF knockdown inhibited the pathological changes of the pancreas and inflammation level in the SAP mouse model. (A) ALYREF mRNA expression in mouse pancreatic tissues was measured by qPCR. (B) Western blot was performed to detect the protein levels of ALYREF in mouse pancreatic tissues. (C, D) H&E staining was performed to evaluate pathological change in pancreatic tissues of mice. (E) Pyroptosis cells in pancreatic tissues of mice were detected by TUNEL assay. (F–H) The levels of inflammatory factors IL-1β, IL-6 and TNF-α in serums of mice were measured using ELISA kits. ***$p < 0.001$ versus the KO-NC or normal group. ###$p < 0.001$ versus the SAP + KO-NC group.

knockdown (Figure 6A). Moreover, GSK significantly increased LDH release suppressed by ALYREF knockdown (Figure 6B). Western blot showed that the protein levels of NLRP3 and CASP1 in the SAP cell model downregulated by ALYREF knockdown were upregulated by GSK treatment (Figure 6C). The CHX chase experiment suggested that with the prolongation of CHX treatment time, the inactivation of the AKT/mTOR pathway was inhibited, but the level of pyroptosis significantly decreased (Figure S1A,B). Additionally, GSK promoted pyroptosis in the SAP cell model suppressed by ALYREF knockdown (Figure 6D). In conclusion, we demonstrated that suppressing the activation of AKT/mTOR signaling pathway promoted pyroptosis inhibited by ALYREF knockdown in the SAP cell model.

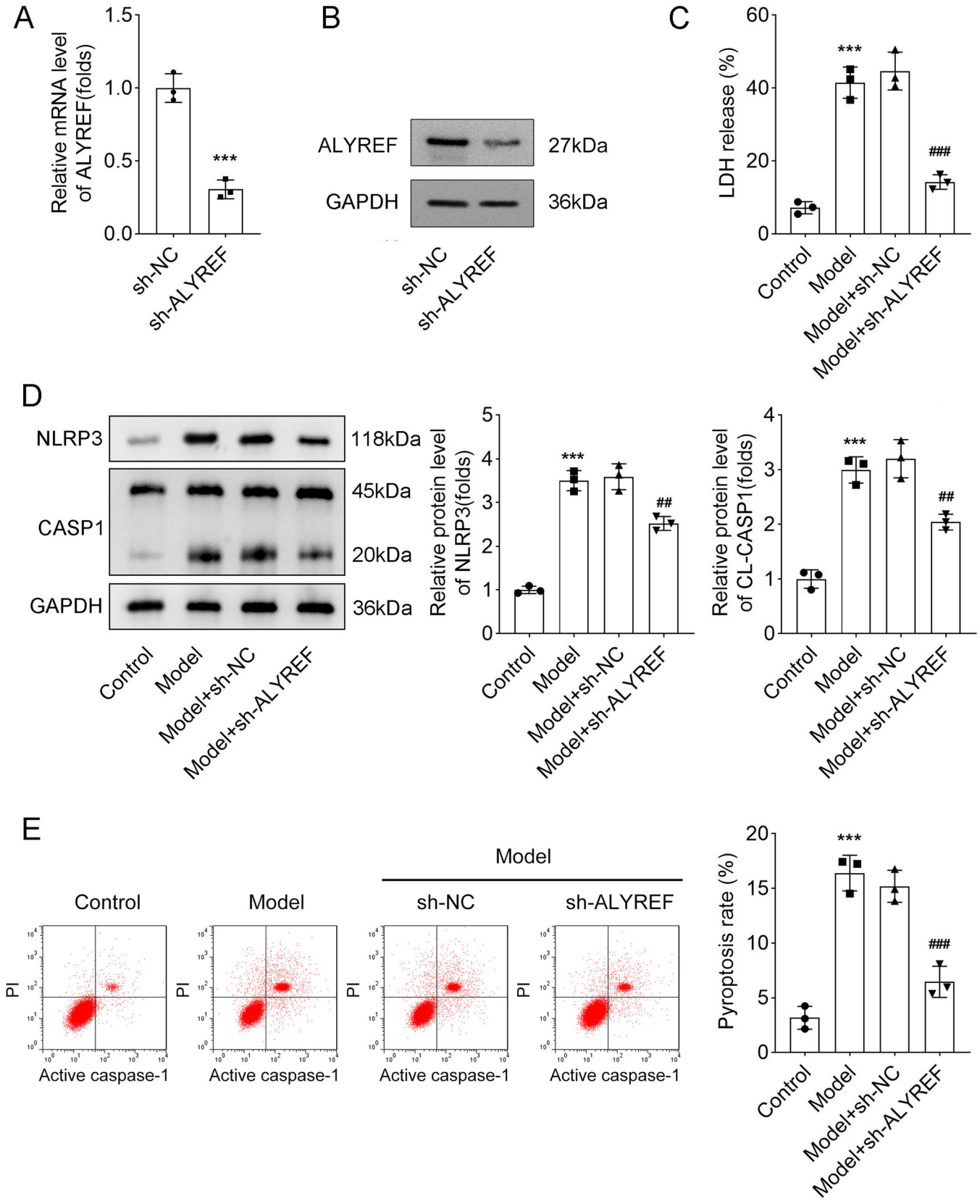

FIGURE 4 | ALYREF knockdown inhibited pyroptosis in the SAP cell model. (A) qPCR measured the expression of ALYREF. (B) The protein levels of ALYREF in 266-6 cells were detected by western blot. (C) LDH release was detected using a LDH cytotoxicity assay kit. (D) Western blot was performed to detect the protein levels of NLRP3 and CASP1. (E) Pyroptosis was evaluated by flow cytometry. ***$p < 0.001$ versus the sh-NC group; ###$p < 0.001$ versus the model+sh-NC group.

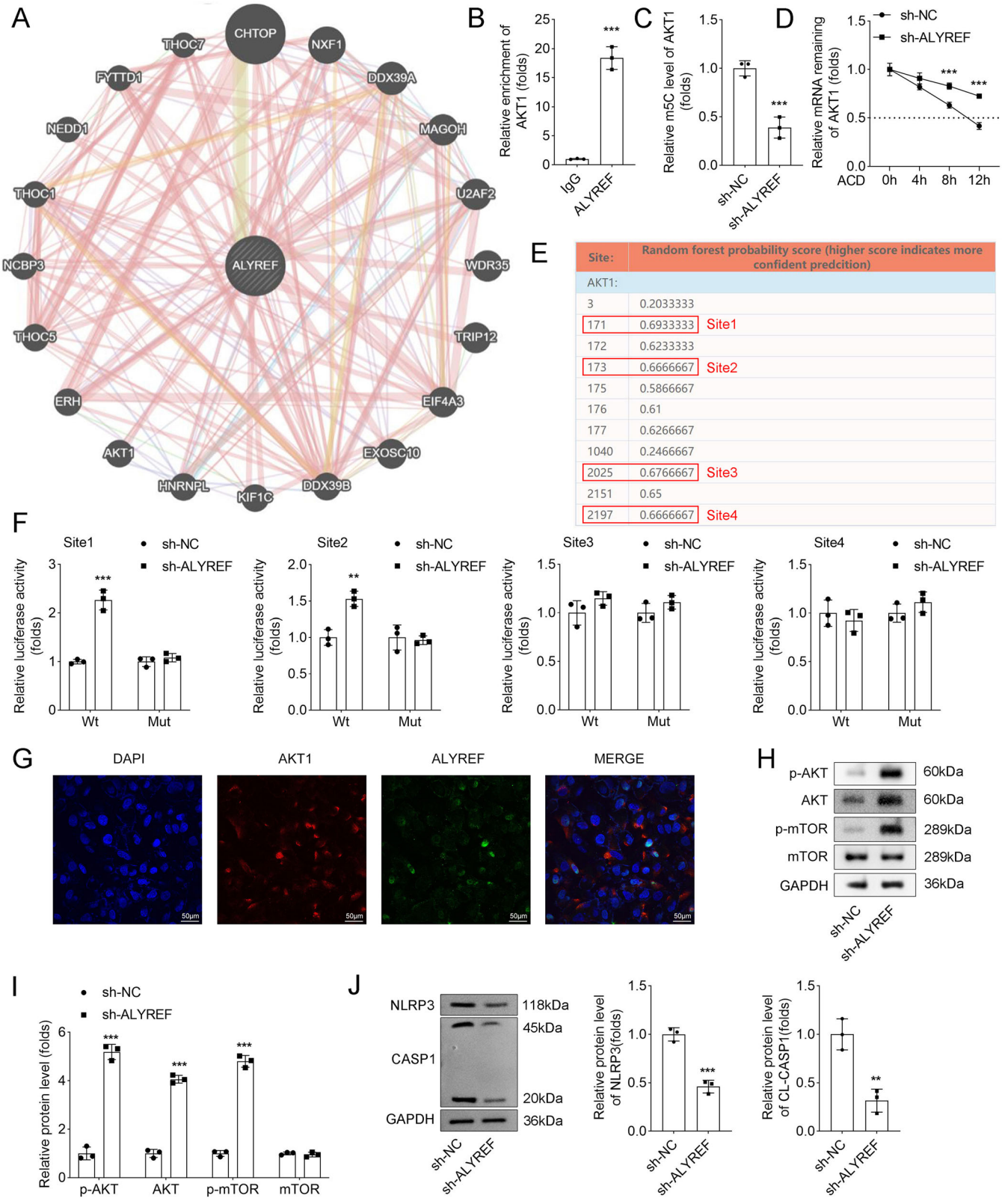

FIGURE 5 | ALYREF knockdown activated AKT/mTOR signaling pathway by inhibiting the m5C modification on AKT1. (A) Genes interacted with ALYREF were predicted using the GeneMANIA database. (B) The interaction between ALYREF and AKT1 was evaluated by RIP. (C) MeRIP was performed to measure the m5C modification on AKT1. (D) The stability of AKT1 mRNA was detected by qPCR before and after treatment of 5 μg/mL actinomycin D for 4, 8 and 12 h. (E) The potential m5C sites of AKT1 were predicted using the RNAm5Cfinder database. (F) Dual luciferase reports were performed to detect the luciferase activity of WT- or Mut-AKT1 in 266-6 cells transfected with sh-NC or sh-ALYREF. (G) The distribution of AKT1 and ALYREF in 266-6 cells was detected by IF staining. (H, I) Western blot was performed to detect the levels of p-AKT, AKT, p-mTOR and mTOR. (J) The protein levels of NLRP3 and CASP1 were detected by western blot. $^{**}p < 0.01$ and $^{***}p < 0.001$ versus the sh-NC group or IgG group.

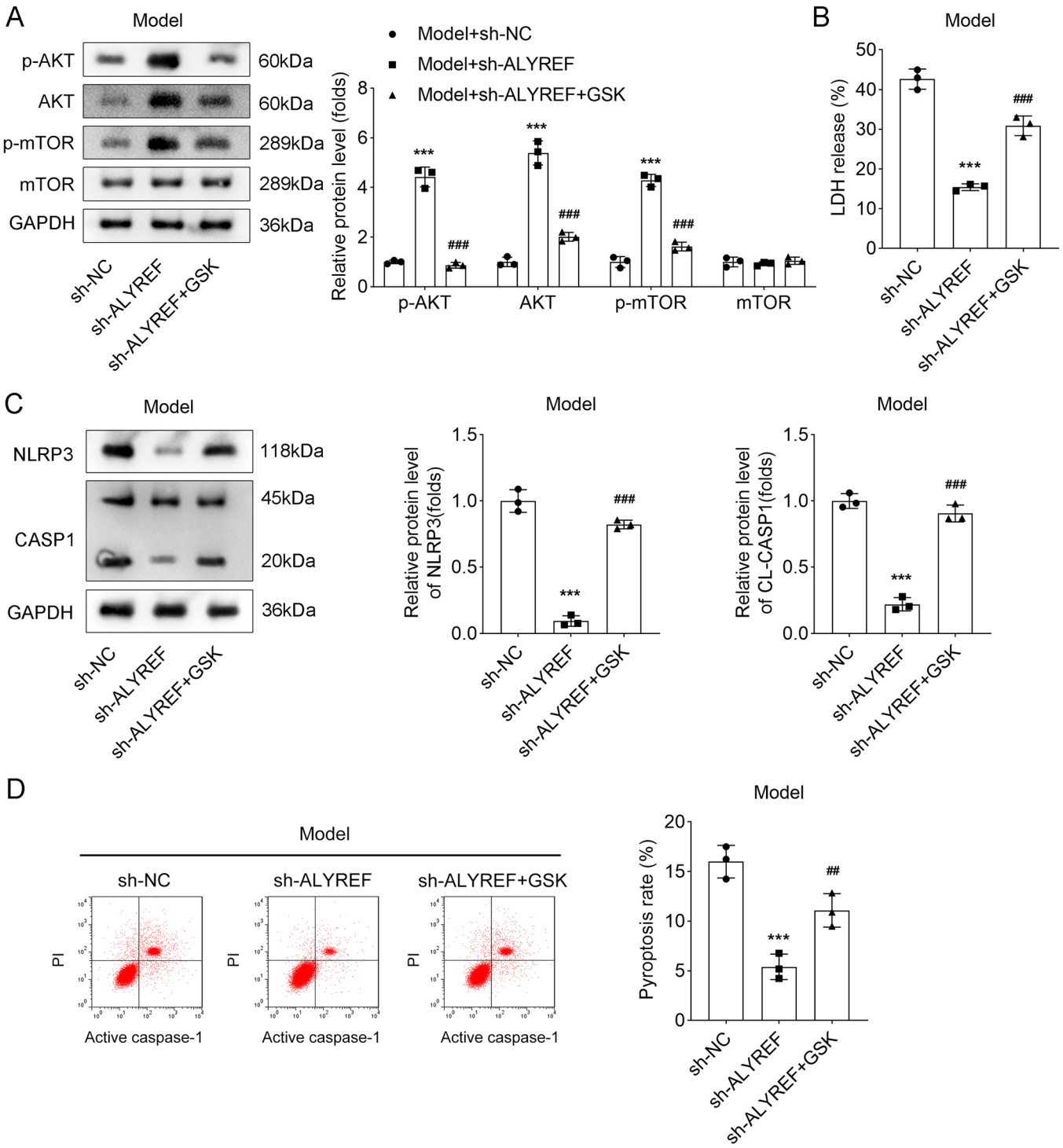

FIGURE 6 | Inhibition of the AKT/mTOR signaling pathway activation promoted pyroptosis in the SAP cell model inhibited by ALYREF knockdown. (A) The protein levels of p-AKT, AKT, p-mTOR and mTOR were detected by western blot. (B) LDH release was detected using a LDH cytotoxicity assay kit. (C) Western blot was performed to detect the protein levels of NLRP3 and CASP1. (D) Pyroptosis was evaluated by flow cytometry. ***$p < 0.001$ versus the sh-NC group; ##$p < 0.01$ and ###$p < 0.001$ versus the sh-ALYREF group.

4 | Discussion

Despite the development and updating of treatments for SAP, it remains a disease with a high mortality and challenging to treat. Pyroptosis has been demonstrated to promote inflammation in SAP, and inhibition of pyroptosis may be an effective therapeutic way to treat SAP. In this study, we investigated the pyroptosis level and the pyroptosis level of SAP and its mechanism, and found that the pyroptosis levels were increased in the in vivo and in vitro SAP models. Moreover, m5C modification and ALYREF expression were upregulated in the SAP cell model, which inhibited the

activation of AKT/mTOR signaling pathway, thereby facilitated pyroptosis.

Excessive inflammation induced by regulatory cell death plays a key role in the pathogenesis of SAP. Numerous studies have investigated the function of apoptosis and ferroptosis in the development of SAP, but the studies about pyroptosis in the pathogenesis of SAP is insufficient [40, 41]. Gao et al. [35] first investigated the crucial role of acinar cell pyroptosis in the pathogenesis of SAP, and found that NLRP3 inflammasome in acinar cells and the activation of GSDMD mediates pyroptosis and systemic inflammation in SAP. Moreover, Ma et al. [22] IL-37 inhibited acinar cell pyroptosis and pathological injury of pancreatic tissue in SAP mouse model. Additionally, inhibition of pyroptosis by GSDMD knockdown or exogenous administration of Salidroside can effectively improve the inflammation level of in vivo SAP model and the pathological injury of pancreatic tissues [10, 23]. These evidence demonstrated that inhibition of pyroptosis is an effective treatment for SAP. In the present study, we demonstrated that the inflammation level and pyroptosis was increased in the in vivo and in vitro SAP model, while ALYREF knockdown improved inflammatory cell infiltration of pancreatic tissues and inflammation level in the SAP mouse model, as well as inhibited pyroptosis in the SAP cell model, indicating that suppression of pyroptosis by inhibiting ALYREF expression is effective on the treatment of SAP.

ALYREF is the reader of m5C modification located in the nucleus specifically recognizing and directly binding to the m5C sites in RNA and facilitates the export of RNA from the nucleus to the cytoplasm [42]. ALYREF is involved in the development of diseases by regulating the stability of mRNA through m5C modification. However, much of the current research on the role of ALYREF in disease has focused on cancers. For example, ALYREF promotes the development of non-small cell lung cancer and urothelial bladder cancer by enhancing m5C modification of target RNA [43, 44]. Notably, He et al. demonstrated that ALYREF is upregulated in abdominal aortic aneurysms and is associated with inflammatory infiltration (CD45+ and CD3+) [45]. However, the role of ALYREF in other inflammatory diseases remains unexplored, and its specific function in SAP pathogenesis has not yet been clearly defined. In this study, we confirmed that m5C modification and ALYREF expression were enhanced in the in vivo and in vitro SAP models. Mechanistically, ALYREF binds to m5C-modified sites on AKT1 mRNA, and ALYREF knockdown protected AKT1 from degradation by exonucleases and enhancing its translation. This process activated the AKT/mTOR pathway, inhibiting pancreatic acinar cell pyroptosis and systemic inflammation. This is the first study to reveal the role of ALYREF in SAP and pyroptosis. The clinical significance of ALYREF lies in its potential as a therapeutic target for SAP. Inhibition of ALYREF could stabilize AKT1 mRNA, thereby suppressing pyroptosis and attenuating SAP severity. Given the limited targeted therapies for SAP, ALYREF represents a promising candidate for precision medicine approaches. Future studies should explore ALYREF's role in patient cohorts and validate its druggability in preclinical models.

AKT/mTOR signaling pathway is highly conserved in eukaryotic cells that promote cell survival, cell growth, and cell cycle progression [46]. Several studies have demonstrated that AKT/mTOR signaling pathway regulates pyroptosis in multiple diseases. Chen et al. [47] revealed that hASCs-derived exosomal miR-155-5p activates the AKT/mTOR signaling pathway and inhibits pyroptosis to improve intervertebral disc degeneration. Moreover, Wei et al. demonstrated that doxorubicin increased pyroptosis and suppressed the activation of PI3K/Akt/mTOR signaling pathway of mice [48]. Ning et al. [49] confirmed that Baicalein inhibited pyroptosis by facilitating autophagy through inhibiting the activation of AKT/mTOR pathway in *Mycobacterium tuberculosis*-infected macrophages. However, the role of AKT/mTOR pathway in pyroptosis of SAP has not been reported. In this study, we demonstrated ALYREF knockdown enhanced the stability of AKT1 mRNA by inhibiting m5C modification on it and thus activating the AKT/mTOR pathway to inhibit pyroptosis, while AKT/mTOR pathway inhibitor reversed these effect. This study provided new evidence for the role of the AKT/mTOR signaling pathway in SAP.

In conclusion, we demonstrated that ALYREF knockdown inhibited pyroptosis in SAP by inhibiting m5C modification on AKT1 to activate the AKT/mTOR pathway. This study may provide a new basis and strategy for the treatment of SAP.

Author Contributions

All authors contributed to the study conception and design. Material preparation, data collection and analysis were performed by Jinlong Wei, Zhenglin Zhang, Jin Wang, Wen Jiang, Long Qian and Maoming Xiong. The first draft of the manuscript was written by Jinlong Wei and all authors commented on previous versions of the manuscript. All authors read and approved the final manuscript.

Ethics Statement

This study was approved by the Ethics Committee of Anhui College of Traditional Chinese Medicine (Approval number: KY-2024-027). All methods were carried out in accordance with relevant guidelines and regulations.

Conflicts of Interest

The authors declare no conflicts of interest.

Data Availability Statement

The datasets used and/or analyzed during the current study are available from the corresponding author on reasonable request.

References

1. A. Leppaniemi, et al., "2019 WSES Guidelines for the Management of Severe Acute Pancreatitis," *World Journal of Emergency Surgery* 14 (2019): 27.

2. H. C. van Santvoort, O. J. Bakker, T. L. Bollen, et al., "A Conservative and Minimally Invasive Approach to Necrotizing Pancreatitis Improves Outcome," *Gastroenterology* 141, no. 4 (2011): 1254–1263.

3. P. K. Garg and V. P. Singh, "Organ Failure Due to Systemic Injury in Acute Pancreatitis," *Gastroenterology* 156, no. 7 (2019): 2008–2023.

4. E. Zerem, "Treatment of Severe Acute Pancreatitis and Its Complications," *World Journal of Gastroenterology* 20, no. 38 (2014): 13879–13892.

5. P. Szatmary, T. Grammatikopoulos, W. Cai, et al., "Acute Pancreatitis: Diagnosis and Treatment," *Drugs* 82, no. 12 (2022): 1251–1276.

6. N. Gliem, C. Ammer-Herrmenau, V. Ellenrieder, and A. Neesse, "Management of Severe Acute Pancreatitis: An Update," *Digestion* 102, no. 4 (2021): 503–507.

7. Y. Rong, J. Ren, W. Song, et al., "Resveratrol Suppresses Severe Acute Pancreatitis-Induced Microcirculation Disturbance Through Targeting SIRT1-FOXO1 Axis," *Oxidative Medicine and Cellular Longevity* 2021 (2021): 8891544.

8. H. Xu, Q. Wen, H. Hu, et al., "Electroacupuncture at ST36 Modulates the Intestinal Microecology and May Help Repair the Intestinal Barrier in the Rat Model of Severe Acute Pancreatitis," *Microbial Biotechnology* 17, no. 2 (2024): e14401.

9. Z. Wang, J. Liu, Y. Wang, et al., "Identification of Key Biomarkers Associated With Immunogenic Cell Death and Their Regulatory Mechanisms in Severe Acute Pancreatitis Based on WGCNA and Machine Learning," *International Journal of Molecular Sciences* 24, no. 3 (2023): 3033.

10. T. Lin, J. Song, X. Pan, et al., "Downregulating Gasdermin D Reduces Severe Acute Pancreatitis Associated With Pyroptosis," *Medical Science Monitor* 27 (2021): e927968.

11. Y. Peng, Y. Yang, Y. Li, et al., "Mitochondrial (mt)Dna-Cyclic Gmp-Amp Synthase (cGAS)-Stimulator of Interferon Genes (STING) Signaling Promotes Pyroptosis of Macrophages via Interferon Regulatory Factor (IRF)7/IRF3 Activation to Aggravate Lung Injury During Severe Acute Pancreatitis," *Cellular & Molecular Biology Letters* 29, no. 1 (2024): 61.

12. X. Wei, F. Xie, X. Zhou, et al., "Role of Pyroptosis in Inflammation and Cancer," *Cellular & Molecular Immunology* 19, no. 9 (2022): 971–992.

13. X. Xia, X. Wang, Z. Cheng, et al., "The Role of Pyroptosis in Cancer: Pro-Cancer or Pro-Host?," *Cell Death & Disease* 10, no. 9 (2019): 650-13.

14. T. Du, J. Gao, P. Li, et al., "Pyroptosis, Metabolism, and Tumor Immune Microenvironment," *Clinical and Translational Medicine* 11, no. 8 (2021): e492.

15. Z. Zhang, Y. Zhang, S. Xia, et al., "Gasdermin E Suppresses Tumour Growth by Activating Anti-Tumour Immunity," *Nature* 579, no. 7799 (2020): 415–420.

16. Y. Fang, S. Tian, Y. Pan, et al., "Pyroptosis: A New Frontier In Cancer," *Biomedicine & Pharmacotherapy = Biomedecine & Pharmacotherapie* 121 (2020): 109595.

17. Z. Rao, Y. Zhu, P. Yang, et al., "Pyroptosis in Inflammatory Diseases and Cancer," *Theranostics* 12, no. 9 (2022): 4310–4329.

18. C. Huang, J. Li, and C. Zhang, "What Role Does Pyroptosis Play in Cancer?," *Molecular Metabolism* 65 (2022): 101587.

19. M. de Carvalho Ribeiro and G. Szabo, "Role of the Inflammasome in Liver Disease," *Annual Review of Pathology: Mechanisms of Disease* 17 (2022): 345–365.

20. R. You, X. He, Z. Zeng, Y. Zhan, Y. Xiao, and R. Xiao, "Pyroptosis and Its Role in Autoimmune Disease: A Potential Therapeutic Target," *Frontiers in immunology* 13 (2022): 841732.

21. Z. Zhaolin, L. Guohua, W. Shiyuan, and W. Zuo, "Role of Pyroptosis in Cardiovascular Disease," *Cell Proliferation* 52, no. 2 (2019): e12563.

22. N. Ma, C. Yuan, J. Shi, et al., "Interleukin-37 Protects Against Acinar Cell Pyroptosis in Acute Pancreatitis," *JCI Insight* 7, no. 21 (2022): e161244.

23. X. Wang, J. Qian, Y. Meng, et al., "Salidroside Ameliorates Severe Acute Pancreatitis-Induced Cell Injury and Pyroptosis by Inactivating Akt/NF-κB and caspase-3/GSDME Pathways," *Heliyon* 9, no. 2 (2023): e13225.

24. T. Lin, M. Peng, Q. Zhu, and X. Pan, "S1PR2 Participates in Intestinal Injury in Severe Acute Pancreatitis by Regulating Macrophage Pyroptosis," *Frontiers in Immunology* 15 (2024): 1405622.

25. P. Haruehanroengra, Y. Y. Zheng, Y. Zhou, Y. Huang, and J. Sheng, "RNA Modifications and Cancer," *RNA Biology* 17, no. 11 (2020): 1560–1575.

26. L. Cui, R. Ma, J. Cai, et al., "RNA Modifications: Importance in Immune Cell Biology and Related Diseases," *Signal Transduction and Targeted Therapy* 7, no. 1 (2022): 334.

27. Q. Tang, L. Li, Y. Wang, et al., "RNA Modifications in Cancer," *British Journal of Cancer* 129, no. 2 (2023): 204–221.

28. L. Zheng, Y. Duan, M. Li, et al., "Deciphering the Vital Roles and Mechanism of m5C Modification on RNA in Cancers," *American Journal of Cancer Research* 13, no. 12 (2023): 6125–6146.

29. K. E. Bohnsack, C. Höbartner, and M. T. Bohnsack, "Eukaryotic 5-methylcytosine (m(5)C) RNA Methyltransferases: Mechanisms, Cellular Functions, and Links to Disease," *Genes* 10, no. 2 (2019): 102.

30. M. A. Khan, M. A. Rafiq, A. Noor, et al., "Mutation in NSUN2, Which Encodes an RNA Methyltransferase, Causes Autosomal-Recessive Intellectual Disability," *American Journal of Human Genetics* 90, no. 5 (2012): 856–863.

31. G. Yu, J. Bao, M. Zhan, et al., "Comprehensive Analysis of m5C Methylation Regulatory Genes and Tumor Microenvironment in Prostate Cancer," *Frontiers in immunology* 13 (2022): 914577-914577.

32. H. Yuan, J. Liu, L. Zhao, et al., "Prognostic Risk Model and Tumor Immune Environment Modulation of m5C-Related LncRNAs in Pancreatic Ductal Adenocarcinoma," *Frontiers in immunology* 12 (2021): 800268.

33. Y. Song, Y. Jiang, L. Shi, et al., "Comprehensive Analysis of Key m5C Modification-Related Genes in Type 2 Diabetes," *Frontiers in Genetics* 13 (2022): 1015879.

34. H. Zheng, Y. Aihaiti, Y. Cai, et al., "The m6A/m1A/m5C-Related Methylation Modification Patterns and Immune Landscapes in Rheumatoid Arthritis and Osteoarthritis Revealed by Microarray and Single-Cell Transcriptome," *Journal of Inflammation Research* 16 (2023): 5001–5025.

35. L. Gao, X. Dong, W. Gong, et al., "Acinar Cell NLRP3 Inflammasome and Gasdermin D (GSDMD) Activation Mediates Pyroptosis and Systemic Inflammation in Acute Pancreatitis," *British Journal of Pharmacology* 178, no. 17 (2021): 3533–3552.

36. L. Meng, H. Wu, J. Wu, et al., "Aberrant CircTMEM45A Facilitates Inflammatory Progression of Esophageal Squamous Cell Carcinoma Through m5C-Mediated NLRP3 Activation," *Cancer Research* 85, no. 14 (2025): 2694–2713.

37. Y. Jin, J. Yao, J. Fu, et al., "ALYREF Promotes the Metastasis of Nasopharyngeal Carcinoma by Increasing the Stability of NOTCH1 mRNA," *Cell Death & Disease* 15, no. 8 (2024): 578.

38. X. Lu, Y. Zhang, R. Wang, and Z. Li, "Ginkgolide B Inhibits EMT and Promotes Pyroptosis in Gastric Cancer via AKT/mTOR Pathway," *Drug Design, Development and Therapy* 19 (2025): 2491–2502.

39. Z. Qiu, J. Ma, X. Zhang, M. Jiao, and L. Zhi, "Electroacupuncture Combined With Trigonelline Inhibits Pyroptosis in Cerebral Ischemia-Reperfusion by Suppressing Autophagy via the PI3K/AKT/mTOR Signaling Pathway," *Brain Research Bulletin* 221 (2025): 111200.

40. J. H. Tan, R. C. Cao, L. Zhou, et al., "ATF6 Aggravates Acinar Cell Apoptosis and Injury by Regulating p53/AIFM2 Transcription in Severe Acute Pancreatitis," *Theranostics* 10, no. 18 (2020): 8298–8314.

41. Y. Liu, H. Cui, C. Mei, et al., "Sirtuin4 Alleviates Severe Acute Pancreatitis by Regulating HIF-1α/Ho-1 Mediated Ferroptosis," *Cell Death & Disease* 14, no. 10 (2023): 694.

42. C. Xue, X. Gu, Q. Zheng, et al., "Alyref Mediates RNA m(5)C Modification to Promote Hepatocellular Carcinoma Progression," *Signal Transduction and Targeted Therapy* 8, no. 1 (2023): 130.

43. N. Wang, R. X. Chen, M. H. Deng, et al., "m5C-dependent Cross-Regulation Between Nuclear Reader ALYREF and Writer NSUN2

Promotes Urothelial Bladder Cancer Malignancy Through Facilitating RABL6/TK1 Mrnas Splicing and Stabilization," *Cell Death & Disease* 14, no. 2 (2023): 139.

44. Q. Yang, M. Wang, J. Xu, et al., "LINC02159 Promotes Non-Small Cell Lung Cancer Progression via ALYREF/YAP1 Signaling," *Molecular Cancer* 22, no. 1 (2023): 122.

45. Y. He, H. Zhang, F. Yin, et al., "Novel Insights into the Role of 5-Methylcytosine RNA Methylation in Human Abdominal Aortic Aneurysm," *Frontiers in Bioscience-Landmark* 26, no. 11 (2021): 1147–1165.

46. A. Glaviano, A. S. C. Foo, H. Y. Lam, et al., "PI3K/AKT/mTOR Signaling Transduction Pathway and Targeted Therapies in Cancer," *Molecular Cancer* 22, no. 1 (2023): 138.

47. D. Chen, X. Jiang, and H. Zou, "Hascs-Derived Exosomal miR-155-5p Targeting TGFβR2 Promotes Autophagy and Reduces Pyroptosis to Alleviate Intervertebral Disc Degeneration," *Journal of Orthopaedic Translation* 39 (2023): 163–176.

48. W. Yu, X. Qin, Y. Zhang, et al., "Curcumin Suppresses Doxorubicin-Induced Cardiomyocyte Pyroptosis via a PI3K/Akt/mTOR-dependent Manner," *Cardiovascular Diagnosis and Therapy* 10, no. 4 (2020): 752–769.

49. B. Ning, J. Shen, F. Liu, H. Zhang, and X. Jiang, "Baicalein Suppresses NLRP3 and AIM2 Inflammasome-Mediated Pyroptosis in Macrophages Infected by Mycobacterium tuberculosis via Induced Autophagy," *Microbiology Spectrum* 11, no. 3 (2023): e0471122.

Supporting Information

Additional supporting information can be found online in the Supporting Information section.

Figure S1: ALYREF knockdown inhibited the inactivation of AKT/mTOR pathway and pyroptosis in the SAP cell model. Western blot was performed to detect (A) the protein and phosphorylation levels of AKT and mTOR and (B) the protein levels of NLRP3 and CASP1. original data.